

Surface-plasmon wave at the planar interface of a metal film and a structurally chiral medium

Akhlesh Lakhtakia

CATMAS—Computational & Theoretical Materials Science Group

Department of Engineering Science and Mechanics

Pennsylvania State University, University Park, PA 16802–6812, USA

Abstract. The solution of a boundary-value problem formulated for a modified Kretschmann configuration shows that a surface-plasmon wave can be excited at the planar interface of a sufficiently thin metal film and a nondissipative structurally chiral medium, provided the exciting plane wave is *p*-polarized. An estimate of the wavenumber of the surface-plasmon wave also emerges thereby.

Keywords: Chiral liquid crystal; Kretschmann configuration; Metal optics; Plasmonics; Sculptured thin film; Structural handedness; Surface plasmon

1 Introduction

The propagation of electromagnetic waves localized to the planar interfaces of bulk metals and bulk dielectric materials can be traced back to a hundred years ago [1]. Called surface-plasmon waves, they attenuate normally away from the interface, and are excited only with evanescent waves [2].

In the Kretschmann configuration, the bulk metal is in the form of a thin film of uniform thickness, bounded on one side by a high-refractive-index dielectric material and on the other side by a low-refractive-index dielectric material. A plane wave is launched in the optically denser dielectric material towards the metal film, in order to excite a surface-plasmon wave at the interface of the metal with the optically rarer dielectric material [3]. The plane wave must be *p*-polarized, The telltale sign is a sharp peak in absorbance (i.e., a sharp trough in reflectance without a compensatory peak in transmittance) as the angle of incidence (with respect to the thickness direction) of the launched plane wave is changed [4]. Because the angle of incidence for exciting the surface-plasmon wave is a delicate function of the constitutive properties of all three materials, surface-plasmon waves in the visible and the near-infrared regimes are exploited for sensing, imaging, and other applications [5, 6].

Generally, the optically rarer medium is homogeneous, normal to its planar interface with the metal film at least within the range of the surface-plasmon field. In this communication, this medium is taken to be continuously nonhomogeneous in the

thickness direction. Specifically, the optically rarer medium is structurally chiral, with the axis of helicoidal nonhomogeneity oriented parallel to the thickness direction. To my knowledge, the solution of the associated boundary-value problem has never been reported before, and its application should draw both chiral liquid crystals [7, Chap. 4] and chiral sculptured thin films [8, Chap. 9] into the plasmonics arena.

The plan of this communication is as follows: Section 2 contains a description of a modified Kretschmann configuration, with the optically rarer medium replaced by a structurally chiral material (SCM) slab of sufficient thickness. The combination of the metal film and the SCM slab is sandwiched between two half-spaces occupied by the same isotropic dielectric material that is optically denser than the chosen SCM. A brief description of the electromagnetic boundary-value problem is also presented. Section 3 contains numerical results to show that a surface-plasmon wave can be excited at the planar interface of a metal film and a structurally chiral medium, provided the incident plane wave is p -polarized.

In the following, an $\exp(-i\omega t)$ time-dependence is implicit, with ω denoting the angular frequency. The free-space wavenumber, the free-space wavelength, and the intrinsic impedance of free space are denoted by $k_0 = \omega\sqrt{\epsilon_0\mu_0}$, $\lambda_0 = 2\pi/k_0$, and $\eta_0 = \sqrt{\mu_0/\epsilon_0}$, respectively, with μ_0 and ϵ_0 being the permeability and permittivity of free space. Vectors are in boldface, dyadics underlined twice; column vectors are in boldface and enclosed within square brackets, while matrixes are underlined twice and similarly bracketed. Cartesian unit vectors are identified as $\hat{\mathbf{u}}_x$, $\hat{\mathbf{u}}_y$ and $\hat{\mathbf{u}}_z$.

2 Theory

In conformance with the Kretschmann configuration for launching surface-plasmon waves, the half-space $z \leq 0$ is occupied by a homogeneous, isotropic, dielectric material described by the relative permittivity scalar ϵ_ℓ . Dissipation in this material is considered to be negligible and its refractive index $n_\ell = \sqrt{\epsilon_\ell}$ is real-valued and positive. The laminar region $0 \leq z \leq L_{met}$ is occupied by a metal with relative permittivity scalar ϵ_{met} . A structurally chiral material occupies the region $L_{met} \leq z \leq L_{met} + L_{scm}$, the dielectric properties of this material being described in the following subsection. Finally, without significant loss of generality in the present context, the half-space $z \geq L_{met} + L_{scm}$ is taken to be occupied by the same material as fills the half-space $z \leq 0$. All constitutive properties generally depend on the angular frequency ω .

A plane wave, propagating in the half-space $z \leq 0$ at an angle $\theta \in [0, \pi)$ to the z axis and at an angle $\psi \in [0, 2\pi)$ to the x axis in the xy plane, is incident on the metal-coated SCM slab. The electromagnetic field phasors associated with the incident plane

wave are represented as

$$\left. \begin{aligned} \mathbf{E}_{inc}(\mathbf{r}) &= (a_s \mathbf{s} + a_p \mathbf{p}_+) e^{i\kappa(x \cos \psi + y \sin \psi)} e^{ik_0 n_\ell z \cos \theta} \\ \mathbf{H}_{inc}(\mathbf{r}) &= \frac{n_\ell}{\eta_0} (a_s \mathbf{p}_+ - a_p \mathbf{s}) e^{i\kappa(x \cos \psi + y \sin \psi)} e^{ik_0 n_\ell z \cos \theta} \end{aligned} \right\}, \quad z \leq 0. \quad (1)$$

The amplitudes of the s - and the p -polarized components of the incident plane wave, denoted by a_s and a_p , respectively, are assumed given, whereas

$$\left. \begin{aligned} \kappa &= k_0 n_\ell \sin \theta \\ \mathbf{s} &= -\hat{\mathbf{u}}_x \sin \psi + \hat{\mathbf{u}}_y \cos \psi \\ \mathbf{p}_\pm &= \mp (\hat{\mathbf{u}}_x \cos \psi + \hat{\mathbf{u}}_y \sin \psi) \cos \theta + \hat{\mathbf{u}}_z \sin \theta \end{aligned} \right\}. \quad (2)$$

The reflected electromagnetic field phasors are expressed as

$$\left. \begin{aligned} \mathbf{H}_{ref}(\mathbf{r}) &= (r_s \mathbf{s} + r_p \mathbf{p}_-) e^{i\kappa(x \cos \psi + y \sin \psi)} e^{-ik_0 n_\ell z \cos \theta} \\ \mathbf{H}_{ref}(\mathbf{r}) &= \frac{n_\ell}{\eta_0} (r_s \mathbf{p}_- - r_p \mathbf{s}) e^{i\kappa(x \cos \psi + y \sin \psi)} e^{-ik_0 n_\ell z \cos \theta} \end{aligned} \right\}, \quad z \leq 0, \quad (3)$$

and the transmitted electromagnetic field phasors as

$$\left. \begin{aligned} \mathbf{H}_{tr}(\mathbf{r}) &= (t_s \mathbf{s} + t_p \mathbf{p}_+) e^{i\kappa(x \cos \psi + y \sin \psi)} e^{ik_0 n_\ell (z - L_\Sigma) \cos \theta} \\ \mathbf{H}_{tr}(\mathbf{r}) &= \frac{n_\ell}{\eta_0} (t_s \mathbf{p}_+ - t_p \mathbf{s}) e^{i\kappa(x \cos \psi + y \sin \psi)} e^{ik_0 n_\ell (z - L_\Sigma) \cos \theta} \end{aligned} \right\}, \quad z \geq L_\Sigma, \quad (4)$$

where $L_\Sigma = L_{met} + L_{scm}$. The reflection amplitudes r_s and r_p , as well as the transmission amplitudes t_s and t_p , have to be determined by the solution of a boundary-value problem.

2.1 Constitutive Relations of the SCM

The frequency-domain electromagnetic constitutive relations of the SCM slab can be written as [8]

$$\left. \begin{aligned} \mathbf{D}(\mathbf{r}) &= \epsilon_0 \underline{\underline{\epsilon}}_{scm}(z) \cdot \mathbf{E}(\mathbf{r}) \\ \mathbf{B}(\mathbf{r}) &= \mu_0 \mathbf{H}(\mathbf{r}) \end{aligned} \right\}, \quad L_{met} \leq z \leq L_\Sigma. \quad (5)$$

The frequency-dependent relative permittivity dyadic $\underline{\underline{\epsilon}}_{scm}(z)$ is factorable as

$$\underline{\underline{\epsilon}}_{scm}(z) = \underline{\underline{S}}_z(z - L_{met}) \cdot \underline{\underline{S}}_y(\chi) \cdot \underline{\underline{\epsilon}}_{scm}^{ref} \cdot \underline{\underline{S}}_y^T(\chi) \cdot \underline{\underline{S}}_z^T(z - L_{met}), \quad L_{met} \leq z \leq L_\Sigma,$$

where the reference relative permittivity dyadic

$$\underline{\underline{\epsilon}}_{scm}^{ref} = \epsilon_a \hat{\mathbf{u}}_z \hat{\mathbf{u}}_z + \epsilon_b \hat{\mathbf{u}}_x \hat{\mathbf{u}}_x + \epsilon_c \hat{\mathbf{u}}_y \hat{\mathbf{u}}_y. \quad (6)$$

The dyadic function

$$\underline{\underline{S}}_z(z) = (\hat{\mathbf{u}}_x \hat{\mathbf{u}}_x + \hat{\mathbf{u}}_y \hat{\mathbf{u}}_y) \cos\left(\frac{\pi z}{\Omega}\right) + h (\hat{\mathbf{u}}_y \hat{\mathbf{u}}_x - \hat{\mathbf{u}}_x \hat{\mathbf{u}}_y) \sin\left(\frac{\pi z}{\Omega}\right) + \hat{\mathbf{u}}_z \hat{\mathbf{u}}_z, \quad (7)$$

contains 2Ω as the structural period and $h = \pm 1$ as the structural handedness parameter; thus, the SCM is helicoidally nonhomogeneous along the z axis. The tilt dyadic

$$\underline{\underline{S}}_y(\chi) = (\hat{\mathbf{u}}_x \hat{\mathbf{u}}_x + \hat{\mathbf{u}}_z \hat{\mathbf{u}}_z) \cos \chi + (\hat{\mathbf{u}}_z \hat{\mathbf{u}}_x - \hat{\mathbf{u}}_x \hat{\mathbf{u}}_z) \sin \chi + \hat{\mathbf{u}}_y \hat{\mathbf{u}}_y \quad (8)$$

involves the angle $\chi \in [0, \pi/2]$. The superscript T denotes the transpose.

2.2 Boundary–Value Problem

The procedure to determine the amplitudes r_s , r_p , t_s , and t_p in terms of a_s and a_p is standard [8]. It suffices to state here that the following set of 4 algebraic equations emerges (in matrix notation):

$$\begin{bmatrix} t_s \\ t_p \\ 0 \\ 0 \end{bmatrix} = [\underline{\underline{K}}]^{-1} \cdot [\underline{\underline{B}}_{scm}] \cdot [\underline{\underline{M}}'_{scm}] \cdot \exp\left(i[\underline{\underline{P}}_{met}]L_{met}\right) \cdot [\underline{\underline{K}}] \cdot \begin{bmatrix} a_s \\ a_p \\ r_s \\ r_p \end{bmatrix}. \quad (9)$$

The procedure to compute the 4×4 matrix $[\underline{\underline{M}}'_{scm}]$ is far too cumbersome for reproduction here, the interested reader being referred to [8, Sec. 9.2.2]. The 4×4 matrix $[\underline{\underline{K}}]$ depends on the refractive index n_ℓ as well as the angles θ and ψ as follows:

$$[\underline{\underline{K}}] = \begin{bmatrix} -\sin \psi & -\cos \psi \cos \theta & -\sin \psi & \cos \psi \cos \theta \\ \cos \psi & -\sin \psi \cos \theta & \cos \psi & \sin \psi \cos \theta \\ -\left(\frac{n_\ell}{\eta_0}\right) \cos \psi \cos \theta & \left(\frac{n_\ell}{\eta_0}\right) \sin \psi & \left(\frac{n_\ell}{\eta_0}\right) \cos \psi \cos \theta & \left(\frac{n_\ell}{\eta_0}\right) \sin \psi \\ -\left(\frac{n_\ell}{\eta_0}\right) \sin \psi \cos \theta & -\left(\frac{n_\ell}{\eta_0}\right) \cos \psi & \left(\frac{n_\ell}{\eta_0}\right) \sin \psi \cos \theta & -\left(\frac{n_\ell}{\eta_0}\right) \cos \psi \end{bmatrix}. \quad (10)$$

The remaining two matrixes appearing in (9) are

$$[\underline{\underline{B}}_{scm}] = \begin{bmatrix} \cos(\pi L_{scm}/\Omega) & -h \sin(\pi L_{scm}/\Omega) & 0 & 0 \\ h \sin(\pi L_{scm}/\Omega) & \cos(\pi L_{scm}/\Omega) & 0 & 0 \\ 0 & 0 & \cos(\pi L_{scm}/\Omega) & -h \sin(\pi L_{scm}/\Omega) \\ 0 & 0 & h \sin(\pi L_{scm}/\Omega) & \cos(\pi L_{scm}/\Omega) \end{bmatrix} \quad (11)$$

and

$$\begin{aligned}
[\underline{\underline{P}}_{met}] &= \begin{bmatrix} 0 & 0 & 0 & \omega\mu_0 \\ 0 & 0 & -\omega\mu_0 & 0 \\ 0 & -\omega\epsilon_0\epsilon_{met} & 0 & 0 \\ \omega\epsilon_0\epsilon_{met} & 0 & 0 & 0 \end{bmatrix} \\
&+ \frac{\kappa^2}{\omega\epsilon_0\epsilon_{met}} \begin{bmatrix} 0 & 0 & \cos\psi\sin\psi & -\cos^2\psi \\ 0 & 0 & \sin^2\psi & -\cos\psi\sin\psi \\ 0 & 0 & 0 & 0 \\ 0 & 0 & 0 & 0 \end{bmatrix} \\
&+ \frac{\kappa^2}{\omega\mu_0} \begin{bmatrix} 0 & 0 & 0 & 0 \\ 0 & 0 & 0 & 0 \\ -\cos\psi\sin\psi & \cos^2\psi & 0 & 0 \\ -\sin^2\psi & \cos\psi\sin\psi & 0 & 0 \end{bmatrix}. \tag{12}
\end{aligned}$$

The solution of (9) yields the reflection and transmission coefficients that appear as the elements of the 2×2 matrixes in the following relations:

$$\begin{bmatrix} r_s \\ r_p \end{bmatrix} = \begin{bmatrix} r_{ss} & r_{sp} \\ r_{ps} & r_{pp} \end{bmatrix} \begin{bmatrix} a_s \\ a_p \end{bmatrix}, \quad \begin{bmatrix} t_s \\ t_p \end{bmatrix} = \begin{bmatrix} t_{ss} & t_{sp} \\ t_{ps} & t_{pp} \end{bmatrix} \begin{bmatrix} a_s \\ a_p \end{bmatrix}. \tag{13}$$

Co-polarized coefficients have both subscripts identical, but cross-polarized coefficients do not. The square of the magnitude of a reflection or transmission coefficient is the corresponding reflectance or transmittance; thus, $R_{sp} = |r_{sp}|^2$ is the reflectance corresponding to the reflection coefficient r_{sp} , and so on. The principle of conservation of energy mandates the constraints $R_{ss} + R_{ps} + T_{ss} + T_{ps} \leq 1$ and $R_{pp} + R_{sp} + T_{pp} + T_{sp} \leq 1$, the inequalities turning to equalities only in the absence of dissipation in the region $0 < z < L_\Sigma$.

3 Numerical Results and Discussion

All eight reflectances and transmittances at the free-space wavelength $\lambda_0 = 633$ nm were calculated as functions of the angles θ and ψ . The SCM was chosen to possess the following parameters: $\epsilon_a = 2.7$, $\epsilon_b = 3.0$, $\epsilon_c = 2.72$, $\chi = 30^\circ$, $\Omega = 200$ nm, and $h = \pm 1$. The relative permittivity of the ambient medium was chosen to be $\epsilon_\ell = 5$, and

that of the metal (typ. aluminum) as $\epsilon_{met} = -56 + i21$. For the chosen constitutive parameters, the constraints $R_{ss} + R_{ps} + T_{ss} + T_{ps} = 1$ and $R_{pp} + R_{sp} + T_{pp} + T_{sp} = 1$ hold in the absence of the metal film.

Figure 1 shows the variations of the reflectances (R_{pp} and R_{sp}), transmittances (T_{pp} and T_{sp}), and the absorbance

$$A_p = 1 - (R_{pp} + R_{sp} + T_{pp} + T_{sp}) \quad (14)$$

with θ when $\psi = 0^\circ$, and the incident plane wave is p -polarized. The SCM is 1-period thick (i.e., $L_{scm} = 2\Omega$), whereas the thickness of the metal film varies from 0 to 20 nm in steps of 5 nm. A rapid increase in the absorbance A_p indicates the excitation of a surface-plasmon wave [9]. The values of θ for maximum A_p are identified for different non-zero values of L_{met} in Fig. 1. For instance, the absorbance equals 0.93 at $\theta = 52.33^\circ$, when $L_{met} = 10$ nm. As L_{met} increases, the maximum-absorbance value of θ decreases slightly, whereas the maximum absorbance decreases as well.

The calculations for Fig. 1 were repeated for higher values of L_{scm}/Ω . As the thickness of the SCM slab was increased, the maximum- A_p value of θ for a specific value of L_{met} began to converge. This is exemplified by the plots of A_p vs. θ in Fig. 2 for $L_{scm}/\Omega = 4$ and Fig. 3 for $L_{scm}/\Omega = 10$. Thus, the maximum value of A_p is 0.975 at $\theta = 51.87^\circ$ in Fig. 2(b) and also at $\theta = 51.81^\circ$ in Fig. 3(b), both for $L_{met} = 10$ nm.

A comparison of the three figures indicates that the 5-period thick SCM slab is sufficiently thick as to be equivalent to a SCM half-space, which would be required in the usual theoretical treatment of the (unmodified) Kretschmann configuration [2]. Parenthetically, the planewave response of a SCM half-space cannot be obtained unless the wavevector of the incident plane wave is aligned parallel to the z axis [10], because a sufficiently general eigenmodal decomposition of the electromagnetic fields is unavailable [8, Chap. 9].

Were the SCM replaced by an isotropic dielectric material of relative permittivity ϵ_{iso} and the metal film were absent, total internal reflection would occur for $\theta \geq \sin^{-1} \sqrt{\epsilon_{iso}/\epsilon_\ell}$. Then, $\sin^{-1} \sqrt{\epsilon_{iso}/\epsilon_\ell}$ is the critical angle and $k_0 \sqrt{\epsilon_{iso}}$ is an estimate of the wavenumber of the surface-plasmon wave [9]. But a simple formulation of a “critical angle” is not possible with the SCM. A useful estimate can, however, be made, by setting $\epsilon_{iso} = \max(\epsilon_a, \epsilon_b, \epsilon_c)$, whereby the “critical angle” equals $\sin^{-1} \sqrt{\epsilon_c/\epsilon_\ell} = 50.77^\circ$ for the chosen parameters. Figures 2(b)–(e) and 3(b)–(e) indicate that the surface-plasmon wave is indeed excited in the neighborhood of this estimate of this “critical angle”, which is also ratified by the plots for $L_{met} = 0$ in Figs. 2(a) and 3(a).

In order to confirm the excitation of a surface-plasmon wave at the interface of the metal and the SCM, the time-averaged Poynting vector $\mathbf{P}(z) = (1/2)\text{Re}[\mathbf{E}(z) \times \mathbf{H}^*(z)]$

was plotted against $z \in (0, L_{met})$ for all calculations reported in the previous figures. Shown in Fig. 4 are the cartesian components of $\mathbf{P}(z)$ vs. z in the metal film, when $\theta = 51.81^\circ$, $L_{met} = 10$ nm, $L_{scm} = 10\Omega$, and all other parameters are the same as for Fig. 3. The magnitude of P_z decreases and that of P_x increases, both monotonically, as one traverses the metal film from the interface with the medium of incidence ($z = 0$) to the interface with the SCM ($z = L_{met}$). Clearly thus, the presence of surface-plasmon wave localized to the interface $z = L_{met}$ is confirmed.

Figure 4 also shows the effects of the anisotropy and the structural handedness of the SCM. These effects are manifested in the y -directed component of $\mathbf{P}(z)$ in the metal film. Were the SCM to be replaced by an isotropic material, this component of $\mathbf{P}(z)$ would be identically zero for all z . Also, the sign of this component depends on whether $h = 1$ or $h = -1$.

Although all numerical results presented were calculated for $\psi = 0^\circ$, calculations were made for other values of ψ as well. No significant effect of ψ on the maximum- A_p value of θ was detected.

Figure 5 shows the variations of the relevant reflectances and transmittances, and of the absorbance

$$A_s = 1 - (R_{ss} + R_{ps} + T_{ss} + T_{ps}), \quad (15)$$

with θ for the same parameters as for Fig. 1, except that the incident plane wave is s -polarized. Evidence of the excitation of a surface-plasmon wave is absent from this figure, just as it would be if the SCM slab were to be replaced by a slab made of an isotropic dielectric material [9]. Calculations for higher values of the ratio L_{scm}/Ω also did not reveal the existence of a surface-plasmon wave for s -polarized incidence.

To conclude, the solution of a boundary-value problem formulated for a modified Kretschmann configuration shows that a surface-plasmon wave can be excited at the planar interface of a sufficiently thin metal film and a nondissipative structurally chiral medium, provided that (i) the incident plane wave is p -polarized, and (ii) the wavenumber (i.e., κ) of the surface-plasmon wave roughly equals $k_0 \sqrt{\max(\epsilon_a, \epsilon_b, \epsilon_c)}$. The estimated wavenumber of the surface-plasmon wave may have to be obtained graphically (by setting $L_{met} = 0$), if $\epsilon_{a,b,c}$ are very different from each other.

Acknowledgment. This work was supported in part by the Charles Godfrey Binder Endowment.

References

- [1] J. Zenneck, Ann. Phys. Lpz. 23 (1907) 846.
- [2] H.J. Simon, D.E. Mitchell, J.G. Watson, Am. J. Phys. 43 (1975) 630.
- [3] E. Kretschmann, H. Raether, Z. Naturforsch. A 23 (1968) 2135.
- [4] T. Turbadar, Proc. Phys. Soc. Lond. 73 (1959) 40.
- [5] J. Homola, S.S. Yee, G. Gauglitz, Sens. Actuat. B: Chem. 54 (1999) 3.
- [6] J.M. Brockman, B.P. Nelson, R.M. Corn, Annu. Rev. Phys. Chem. 51 (2000) 41.
- [7] S. Chandrasekhar, Liquid Crystals. 2nd ed., Cambridge University Press, Cambridge, United Kingdom, 1992.
- [8] A. Lakhtakia, R. Messier, Sculptured Thin Films: Nanoengineered Morphology and Optics, SPIE Press, Bellingham, WA, USA, 2005.
- [9] M. Mansuripur, L. Li, OSA Opt. Photon. News 8 (1997) 50 (May issue).
- [10] A. Lakhtakia, M.W. McCall, J. Modern Opt. 49 (2002) 1525.

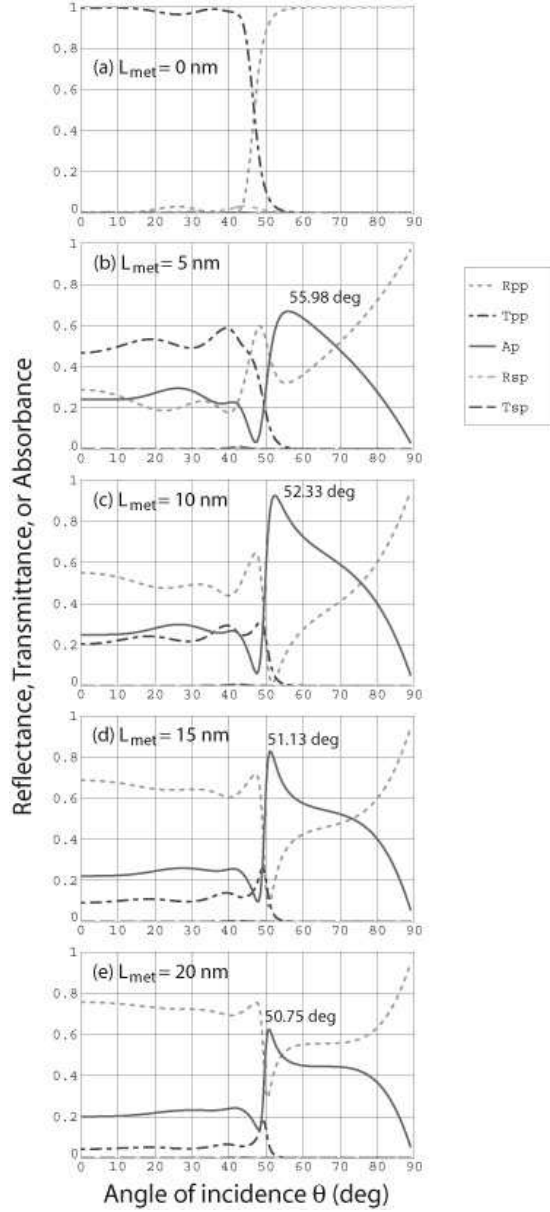


Figure 1: Reflectances (R_{pp} and R_{sp}), transmittances (T_{pp} and T_{sp}), and the absorbance as functions of θ when $\psi = 0^\circ$, $\lambda_0 = 633$ nm, and the incident plane wave is p -polarized. The SCM is described by the following parameters: $\epsilon_a = 2.7$, $\epsilon_b = 3.0$, $\epsilon_c = 2.72$, $\chi = 30^\circ$, $\Omega = 200$ nm, $h = \pm 1$, and $L_{scm} = 2\Omega$. The relative permittivity of the metal is $\epsilon_{met} = -56 + i21$, and that of the ambient medium is $\epsilon_\ell = 5$. (a) $L_{met} = 0$, (b) $L_{met} = 5$ nm, (c) $L_{met} = 10$ nm, (d) $L_{met} = 15$ nm, and (e) $L_{met} = 20$ nm. The values of θ for maximum A_p are identified for different non-zero values of L_{met} in the plots.

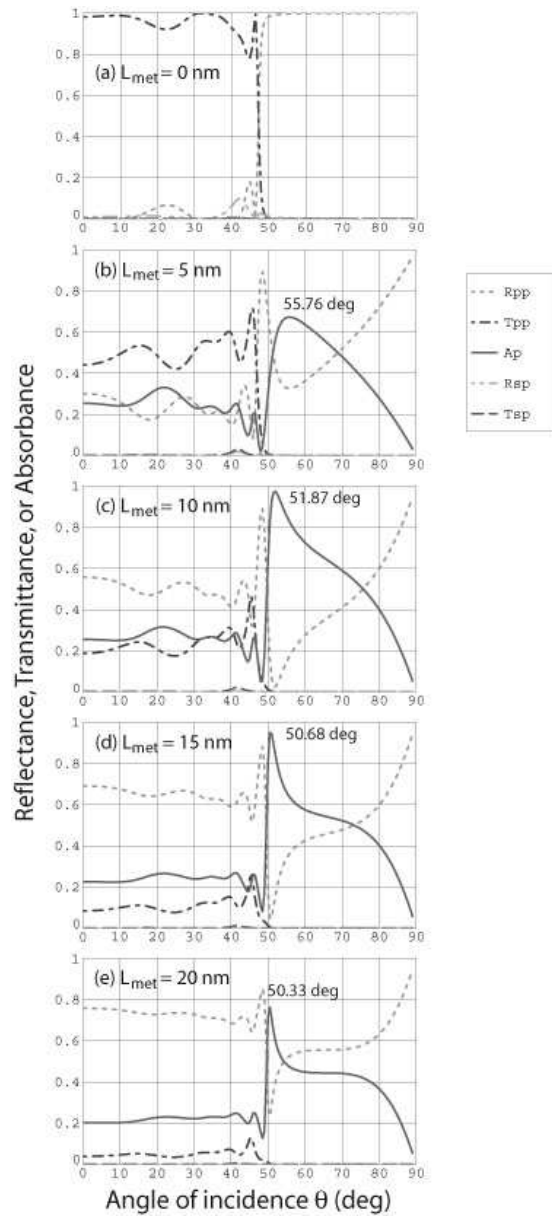


Figure 2: Same as Fig. 1, except that $L_{scm} = 4\Omega$.

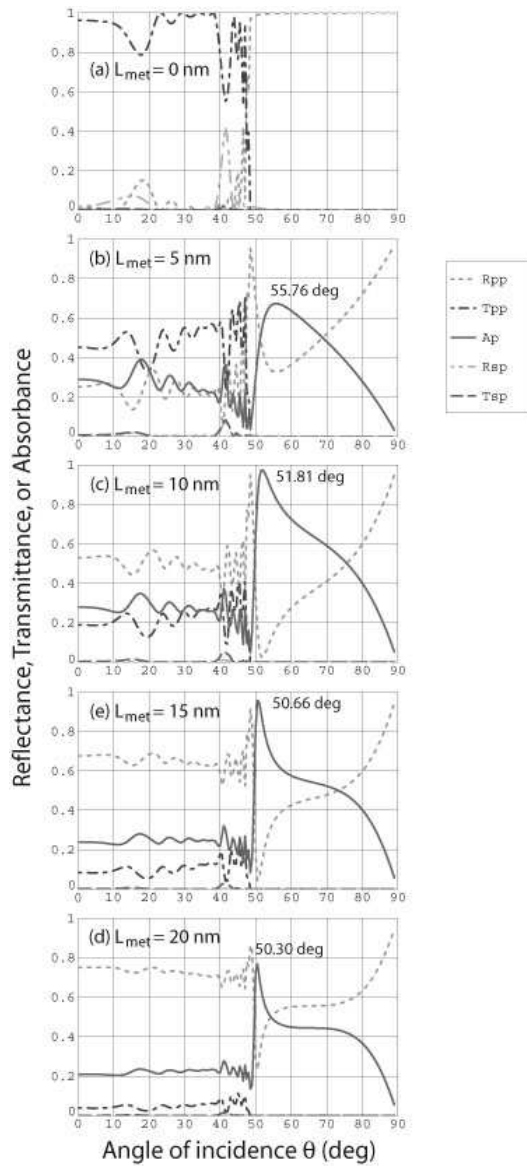


Figure 3: Same as Fig. 1, except that $L_{sem} = 10\Omega$.

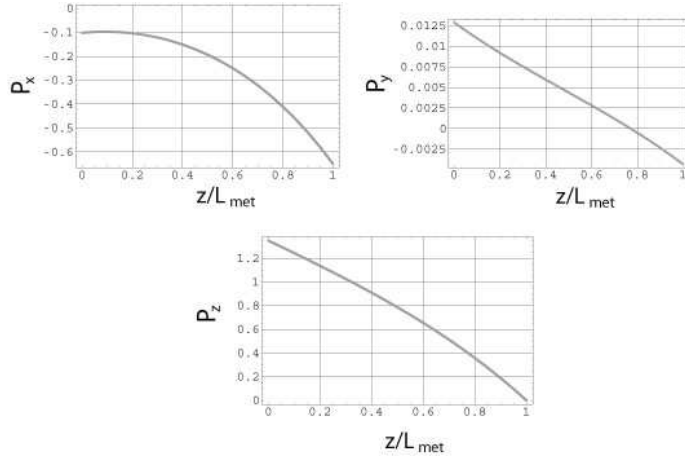


Figure 4: Cartesian components of the time-averaged Poynting vector $\mathbf{P}(z)$ in the metal film vs. $z \in (0, L_{\text{met}})$ when a surface-plasmon wave has been excited. The conditions are the same as for Fig. 3(c), except that $h = 1$. For $h = -1$, the y -directed component of $\mathbf{P}(z)$ is different in sign but not in magnitude.

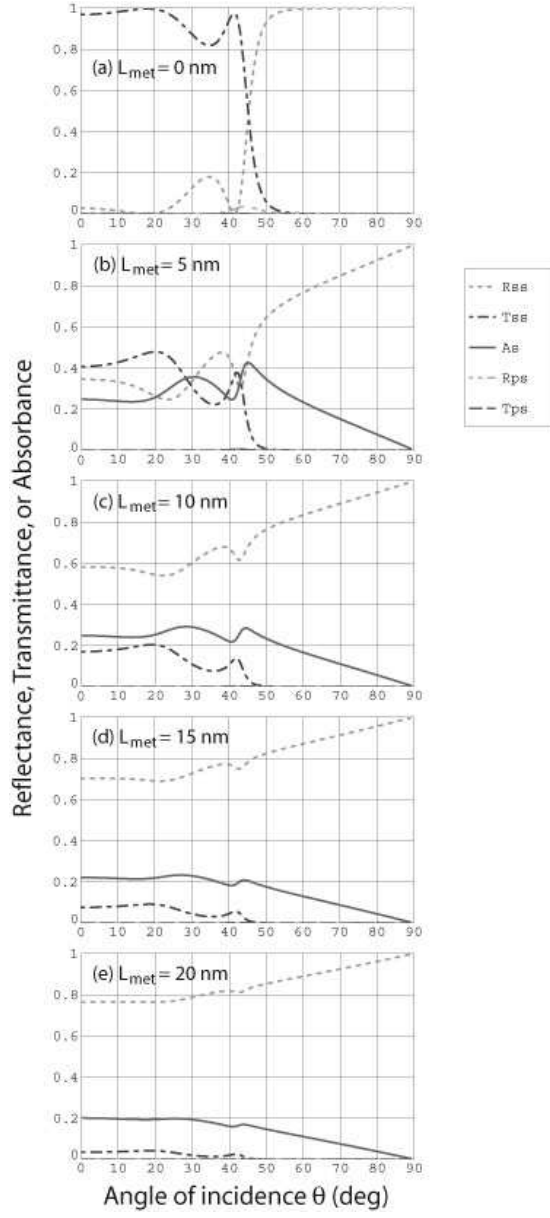


Figure 5: Reflectances (R_{ss} and R_{ps}), transmittances (T_{ss} and T_{ps}), and the absorbance as functions of θ when $\psi = 0^\circ$, $\lambda_0 = 633$ nm, and the incident plane wave is s -polarized. The SCM is described by the following parameters: $\epsilon_a = 2.7$, $\epsilon_b = 3.0$, $\epsilon_c = 2.72$, $\chi = 30^\circ$, $\Omega = 200$ nm, $h = \pm 1$, and $L_{scm} = 2\Omega$. The relative permittivity of the metal is $\epsilon_{met} = -56 + i21$, and that of the ambient medium is $\epsilon_\ell = 5$. (a) $L_{met} = 0$, (b) $L_{met} = 5$ nm, (c) $L_{met} = 10$ nm, (d) $L_{met} = 15$ nm, and (e) $L_{met} = 20$ nm.